NANO LETTERS

2008
Vol. 8, No. 7
1809-1812

Electrical and Optical Transport of GaAs/Carbon Nanotube Heterojunctions

Chen-Wei Liang* and Siegmar Roth

Max-Planck Institute for Solid State Research, Heisenbergstrasse 1, D-70569 Stuttgart, Germany

Received January 22, 2008; Revised Manuscript Received April 4, 2008

ABSTRACT

Heterojunctions consisting of nanotubes and an industrialized semiconductor−GaAs have been produced, and their transport properties were studied. We found that the p-doped GaAs forms an ohmic contact with a nanotube but the n-doped GaAs/nanotube heterojunction is rectifying. Analysis of measurement results at various temperatures shows that tunneling transport plays an important role. We also observed photovoltaic effects in n-GaAs/nanotube junction with the illumination of a green laser or desk lamp.

The interface plays an important role in naonotechnology. For the mechanical, chemical, electrical, or biological properties of a system consisting of both macro- and microscale materials, the interface is often a determinant factor.[1–3] When applying nanotechnology as a tool for cross-discipline research, knowledge of the interface is essential.[4] Carbon nanotube (CNT), a symbolic nanomaterial, possesses unique electrical properties, being an ideal candidate for various components in modern electronics.[5] Depending on the crystal structure, CNTs have a dual electrical property: semiconducting and metallic.[6] Its electrical transport is ballistic up to room temperature, making the material ideal for electronics applications.[7–9] To develop CNT electronics research from science to technology, detailed information about the electrical characteristics of the interfaces between nanotubes and other materials is not trivial. Most of the CNT-based electronics nowadays are built with metallic contacts, where the nanotube/metal interfaces have been studied throughout. But from the history of the semiconductor industry, people have learned that the semiconductor heterostructures have a very wide range of applications, e.g., high-speed computation, solar cells, and high-frequency communication. However, due to the extreme size of nanotubes and the limited applicable process technologies, often is it difficult to contact a single nanotube with other materials to investigate their interfaces (except metal, which can be made by evaporator). Confronted by this issue, we have designed a simple structure for the study of heterojunctions between semiconductor (GaAs) and nanotube (single-walled carbon nanotube, SWNT). GaAs is selected because of its well-developed industrial application and better, compared with Si, electrical performance in certain aspects like higher carrier mobility.

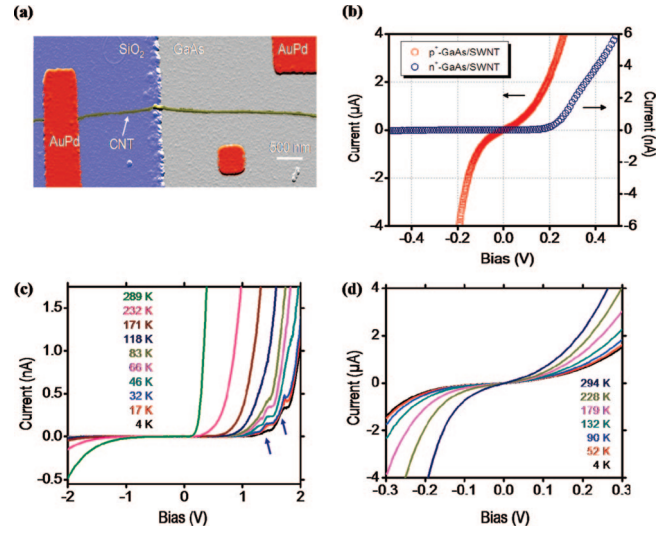

Figure 1. (a) Colored AFM image of an GaAs/SWNT heterjunction. (b) Comparison of the $I-V_{bi}$ curves of n- and p-GaAs/SWNT devices. To the extended voltage range, the current amount of n-GaAs/SWNT at forward bias (2 V, 107 nA) is 3 orders of magnitude larger than it is at reverse bias (−2 V, −485 pA). For p-GaAs/SWNT, the current at both voltage polarities was observed having comparable values (−20.5 μA at −0.3 V; 5.4 μA at 0.3 V) instead of being strongly blocked. (c) $I-V_{bi}$ curves of n-GaAs/SWNT at different temperatures. Arrows point out the staircase-like structure as a consequence of the Coulomb blockade. (d) Temperature-dependent $I-V_{bi}$ curves of the p-GaAs/SWNT heterojunction.

Figure 1a shows the prototype of the GaAs/SWNT heterojunction. A SWNT lies on a highly doped GaAs substrate with an end isolated by a thin insulating layer. The sample preparation began with chips (4 × 4 mm^2) sliced from the GaAs wafer, which was prepatterned with metal markers by e-beam lithography (EBL). Substrates were then

* Corresponding author, cw.liang@fkf.mpg.de.

10.1021/nl0802178 CCC: $40.75
Published on Web 06/05/2008

half-covered with thermal-evaporated SiO_2 (100 nm) via optical lithography. Laser-ablated SWNTs were suspended in a 1% aqueous solution of sodium dodecyl sulfate and transferred onto the GaAs substrates. After the nanotube lying across the edge of SiO_2 was located by atomic force microscopy (AFM), a second EBL was applied to make the electrical contacts (AuPd). There are two electrodes for each GaAs/SWNT junction. One caps the nanotube (the part on the SiO_2 layer) and the other contacts the GaAs substrate. This assures that current goes through the GaAs/SWNT interface. Similar devices were reproduced on both n- and p-doped GaAs (five devices on n-doped GaAs and three on p-doped GaAs).

The current−voltage ($I-V_{bi}$) characteristics of the n-doped GaAs/SWNT and p-doped GaAs/SWNT heterojunctions (denoted as n-GaAs/SWNT and p-GaAs/SWNT, respectively) are shown in Figure 1b. A rectifying behavior is observed in n-GaAs/SWNT: Current is blocked when the SWNT is biased negatively but starts to increase while the polarity is switched to the opposite. Therefore the device is at *forward* (*reverse*) bias when the voltage applied to SWNT is positive (negative). There is a voltage threshold of 0.2 V, until which the current does not increase, at the positive bias. This indicates a built-in electrical field at the interface between n-GaAs and SWNT. Responses to illumination from the n-GaAs/SWNT are then expected accordingly. Contrary to n-GaAs/SWNT, the p-GaAs/SWNT heterojunction shows an ohmic-like behavior instead of rectifying current. This clearly shows a different transport mechanism inside the p-GaAs/SWNT from the n-GaAs/SWNT.

Figure 1c shows that the n-GaAs/SWNT junction is rectifying in the temperature range from room temperature (RT) to 4 K with a decrease of forward current from 107 to 1.5 nA at 2 V. Meanwhile, the threshold voltage increases from 0.2 to 1 V. Staircase-like curves are observed in the forward current at the temperature equal or lower than 66 K. This is resulted from the effect of Coulomb blockade, a typical signature of single electron tunneling in the low-dimensional system.[10] On the other hand, the p-GaAs/SWNT holds the ohmic behavior also from RT down to 4 K (Figure 1d). The $I-V_{bi}$ curve is symmetrical to the zero bias up to 132 K. The conductance at 4 K is 4.53 μS (0.12 e^2/h) at both $\pm$ 0.3 V but is 18 μS (0.46 e^2/h) for −0.3 V and 68.3 μS (1.76 e^2/h) for 0.3 V at RT. Due to the high conductance of the p-GaAs/SWNT junction, p-GaAs, like (Ga,Mn)As, has been proposed as a contact material for CNT field-effect transistors (CNTFETs) in addition to metals.[11] It should be emphasized that although the same behaviors (rectifying for n-GaAs/SWNT and ohmic for p-GaAs/SWNT) as well as their temperature dependence have been observed in all of our devices, the measured values are not always identical. This is due to the variation of the diameter, length, contact area with GaAs and the metal−contact resistance of the nanotubes.

The reproduction of the rectifying behaviors from all of the n-GaAs/SWNT heterojunctions indicates the nanotubes belong to the same type and the their polarity shows that it

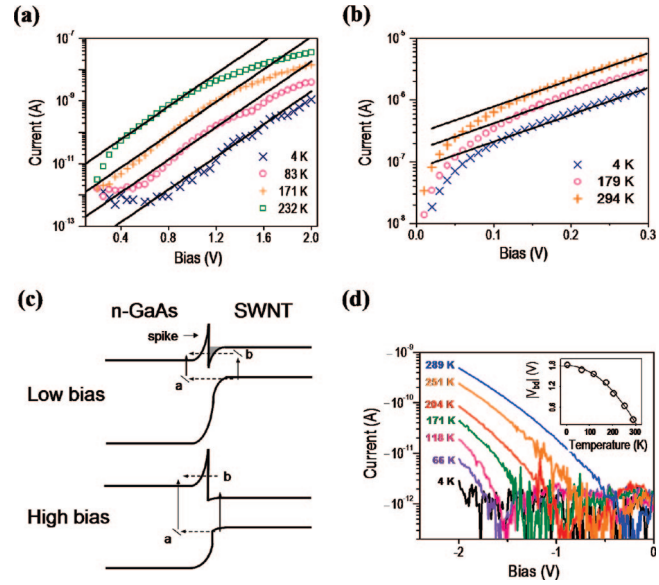

Figure 2. Logarithmic $I-V_{bi}$ curves of the GaAs/SWNT heterojunctions and the tunneling processes: (a) n-GaAs/SWNT junction; (b) p-GaAs/SWNT. Each panel shows the $\log(I)-V$ curves of the GaAs/SWNT heterojunctions at temperature from 4 K to RT in the forward-bias regime. The black lines are the calculated curves using the tunneling transport model. (c) Tunneling processes of the high- and low-bias transport through the n-GaAs/SWNT junction. (d) The $\log(I)-V_{bi}$ curves of the n-GaAs/SWNT junctions in the reverse-bias regime. Inset: absolute values of the breakdown voltage V_{bd} as a function of temperature.

is holes transported in the nanotubes. Hole transport is a distinct feature of semiconducting nanotubes due to their near ohmic contacts with high work function metals like Au or Pd.[8,12] If the nanotube is metallic, the device is then modeled as metal/n-GaAs/metal, where the transport should be dominated by electrons instead of holes. As for the p-GaAs/SWNT, although the current is larger when the p-GaAs is biased positively, indicating its prohole transport mechanism, it is not sufficient to conclude the type of the nanotube because hole transport may exist in either semiconductor/p-GaAs/metal (with a semiconducting nanotube) or metal/p-GaAs/metal (with a metallic nanotube).

The logarithmic version of the $I-V_{bi}$ curves at various temperatures, as shown in panels a and b of Figure 2, reveals the transport details. According to the theory of thin-film semiconductor heterojunctions, two possible models account for the transport mechanism: the thermionic and the tunneling ones.[13,14] The mathematical formulations of the former and the latter are $\log(I) = \log(I_0) + qV_{bi}/kT$ and $\log(I) = \log(I_0) + \alpha V_{bi}$, respectively, where k is the Boltzmann constant, q is the electron charge, I_0 is the saturation current extrapolated from the logarithmic $I-V_{bi}$ curve, and α is a constant related to the tunneling barrier of the junction. The determinant difference between the two mechanisms is the temperature dependence of the slope of the $\log(I)-V_{bi}$ curve. The slope is temperature dependent in the thermionic model but is insensitive to the temperature in the tunneling model. It is noticed that the slope of the curves in both panels a and b of Figure 2 are not sensitive to the temperature. This ascribes the transport of the GaAs/SWNT heterojunctions to the

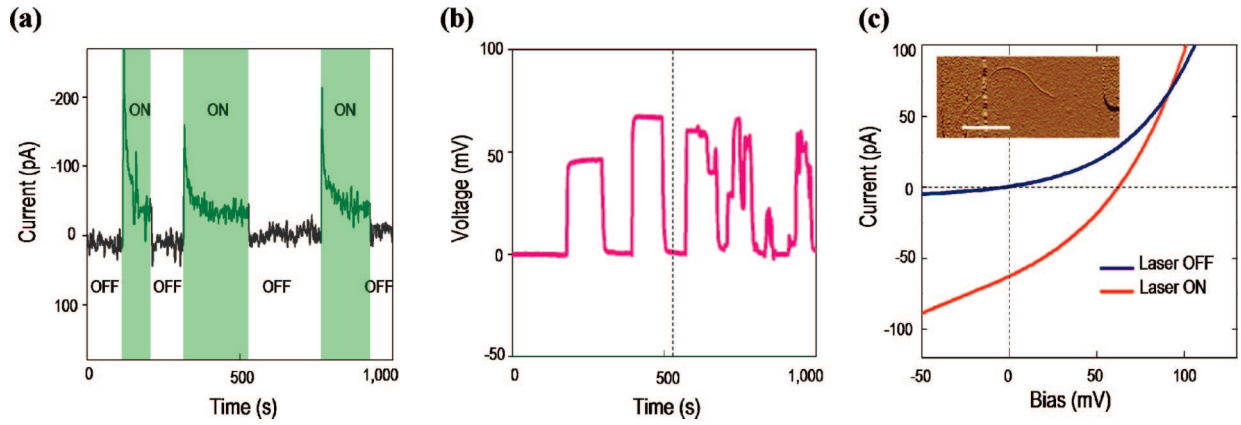

Figure 3. (a) Real-time record of the I_{sc} of a n-GaAs/SWNT device illuminated by a green laser spot (wavelength, 532 nm; power, 10 mW; diameter, 1 mm). (b) Real-time record of the V_{oc} with the shift of the position of the laser spot. In the first half of the measuring period (prior to the time marked by the dashed line) the spot was moved completely inside/outside the area with metal markers (active area, where the devices are made). No V_{oc} was observed while the laser spot was positioned outside the active area. Later than the marked time, the spot was shacked at the vicinity of the active area. An irregular response of the V_{oc} was then observed. (c) $I-V_{bi}$ curves with and without laser illumination. In this measurement, I_{sc} and V_{oc} are 62 pA and 72 mV, respectively. Inset is the AFM image of the tested device. The scale bar represents 1 μm.

tunneling model. Calculation based on the above formula for tunneling transport agrees with the experimental results well. However, data points of the n-GaAs/SWNT junction deviate from the theoretical curves at larger bias (>1 V) and higher temperatures (171 and 232 K). To explain the deviation, a tunneling model introduced by Zeidenbergs et al. is adopted.[14] This approach is based on the Anderson model[15] of the thin-film semiconductor heterojunction, which introduces a spike structure at the interface of the heterojunction. Zeidenbergs et al. argued that when tunneling is the dominating transport mechanism, the tunneling barriers of a degenerate semiconductor heterojunction at high and low bias are different. As illustrated in the Figure 2c, holes in the SWNTs can tunnel across the n-GaAs/SWNT through two routes: (process a) tunneling from the SWNT valence band edge to the interband states in the n-GaAs and then recombining with electrons in the conduction band of n-GaAs, or (process b) jumping from the valence band to the interband states of SWNT and then tunneling through both the inversion layer (gray area) and the spike to the GaAs conduction band. The difference between the low/high-bias transport is the existence of the inversion layer. The inversion layer is negligible at high bias but is not at low bias. This results in a different tunneling barrier seen by electrons, causing a different slop of the $\log(I)-V_{bi}$ curve (denoted as α previously) for low and high bias regions. Since the calculations in Figure 2a use the same α value throughout the whole bias range, deviation occurs.

The tunneling transport of the n-GaAs/SWNT junction is further characterized by the transport results at reverse bias region. When the reverse bias is sufficiently low (smaller than the so-called breakdown voltage V_{bd}), a sharp decrease of the current is observed. This is often called "junction breakdown". Figure 2d shows the breakdwon regime of the n-GaAs/sWNT at different temperature. Two main mechanisms account for the breakdown phenomena: the Zener breakdown and the avalanche breakdown. The Zener breakdown comes from the direct tunneling through depletion region at the junction. The amount of the reverse current arises because of the thinning of the depletion region at lower bias. However, the avalanche breakdown resulted from the impact ionization: when the electrons are energized by the bias voltage and injected into the depletion layer, they will collide with atoms and induce ionization thereof. A distinction between the two mechanisms is their temperature dependence.[16] The breakdown voltage is lower at higher temperature for the avalanche breakdown because at high temperature the energy of the electrons is relaxed by the phonons in the depletion region. Opposite to the avalanche breakdown, the breakdown voltage increases at higher temperature in the case of Zener breakdown. This is because the semiconductor bandgap decreases at high temperature,[17] resulting in a reduction of the tunneling barrier at the depletion region.[16] The breakdown behavior of the n-GaAs/SWNT (Figure 2d) shows a V_{bd} increase with increasing temperature and is then ascribed to the Zener breakdown. The temperature dependence of the V_{bd} (in absolute value) is plotted in the inset of Figure 2d. The decrease of the absolute value of V_{bd} is linear at higher temperatures (>100 K) but nonlinear at lower temperatures. This may be explained by the decrease of the bandgap that is nonlinear at low temperature and linear at sufficiently high temperature for both GaAs and SWNT.[18,19]

In addition to the above analysis based on the band structure of the semiconductor heterojunction, some other factors may contribute to the tunneling behavior of the GaAs/SWNT junction. From the theoretical point of view, the adoption of the semiclassic model should be considered as a qualitative approach rather than a complete interpretation because the GaAs/SWNT junction is not an infinitive two-dimensional interface due to the small diameter of the nanotubes. Therefore it would be necessary to incorporate the low-dimensional theory for a more detailed anaysis. In the case of carbon nanotube field-effect transtor (CNTFET), light electron effective mass in nanotubes is proposed to be the main reason of tunneling transport in CNTFETs.[20]

Further, the native oxide layer of GaAs (Ga_2O_3, 1−2 nm) may also contribute to the tunneling barrier in this experiment.

The n-GaAs/SWNT junction was further characterized electrically with illumination, and a photovoltaic effect was observed. The device responses to the green laser shining with a short-circuit current I_{sc}. Switching on/off the laser causes the generation/annihilation of I_{sc} alternatively (Figure 3a). In addition to the I_{sc}, the open-circuit voltage V_{oc} was also measured. Figure 3b shows that V_{oc} increases (vanishes) while moving the laser spot close to (away from) the position of the tested nanotube on the substrate. This confirms that the photovoltaic effect is not induced spuriously from other places remote to the device. The $I-V_{bi}$ curves with and without illumination are compared in Figure 3c, from which a filling factor f of 0.33 is obtained. The short-circuit current density J_{sc} of 2 A/cm^2 is estimated via a methodology of using projected area, which is commonly applied to the nanoscale photovoltaic devices.[21–23] The photovoltaic efficiency of the n-GaAs/SWNT junction is then calculated and found to be 3.8% by the conversion equation:

$$\eta = \frac{fJ_{sc}V_{oc}}{P_{input}}$$

where η is the efficiency, f is the filling factor, and P_{input} is the input power density obtained by dividing the total laser power with its spot area. Beside the green laser, photovoltaic effects have also been observed when illuminating the same device with a regular desk lamp (Supporting Information-Figure S1).

According to the results of the optical transport, n-GaAs/SWNT heterojunctions have potential for energy-transformation technologies such as solar cells. There are several foreseeable advantages when using SWNTs as an active component in a solar cell. For example, its variable bandgap increases the absorption spectrum by forming different barrier heights at the semiconductor/nanotube interface; its nanoscale size multiplies the light-sensing area enormously; its flexibility facilitates the integration of the cell into other systems. However, these benefits would not be available until some technical challenges are overcome, e.g., separation of semiconducting/metallic nanotubes or a practical design of the device structure.

In conclusion, both n- and p-GaAs/SWNT heterojunctions have been prepared and their transport properties have been investigated systematically. The n-GaAs/SWNT junction showed a strong rectifying behavior, while ohmic-like contact formed in the p-GaAs/SWNT junction. Photovoltaic effects were observed in the n-GaAs/SWNT junction when the device is illuminated. This experiment lays the groundwork for further studies on semiconductor/nanotube hybrid devices, which may open the access to new technologies: the p-GaAs could be used as a ohmic-contact material for SWNT electronics; n-GaAs/SWNT junctions can be applied as either diode components for high-frequency communication or photovoltaic devices for renewable energy technologies.

Acknowledgment. We thank xlith for preparing the marker system. This work was supported by the CANAPE project and Deutscher Akademischer Austauch Dienst (DAAD).

Supporting Information Available: Photovoltaic effects of n-GaAs/SWNT from different light sources. This material is available free of charge via the Internet at http://pubs.acs.org.

References

(1) Suresh, S. *Science* **2001**, *292*, 2447.
(2) Adams, D. M.; Brus, L.; Chidsey, C. E. D.; Creager, S.; Creutz, C.; Kagan, C. R.; Kamat, P. V.; Marya Lieberman, M.; Lindsay, S.; Marcus, R. A.; Metzger, R. M.; Michel-Beyerle, M. E.; Miller, J. R.; Newton, M. D.; Rolison, D. R.; Otto Sankey, O.; Kirk, S.; Schanze, K. S.; Yardley, J.; Zhu, X. *J. Phys. Chem. B* **2003**, *107*, 6668.
(3) Medintz, I.; Uyeda, H.; Goldman, E.; Mattoussi, H. *Nat. Mater.* **2005**, *4*, 435.
(4) Patolsky, F.; Timko, B.; Zheng, G.; Lieber, C. M. *MRS Bull.* **200**, *732*, 142.
(5) Avouris, P. *MRS Bull.* **2004**, *29*, 430.
(6) Saito, R.; Dresselhaus, G.; Dresselhaus, M. S. *Physical Properties of Carbon Nanotubes*; Imperial College Press: London, 1998.
(7) White, C. T.; Todorov, T. N. *Nature* **1998**, *393*, 240.
(8) Javey, A.; Guo, J.; Wang, Q.; Lundstrom, M.; Dai, H. *Nature* **2003**, *424*, 654.
(9) Frank, S.; Poncharal, P.; Wang, Z. L.; de Heer, W. A. *Science* **1998**, *280*, 1744.
(10) Tans, S. J.; Devoret, M. H.; Dai, H.; Thess, A.; Smalley, R. E.; Geerligs, L. J.; Dekker, C. *Nature* **1997**, *386*, 474.
(11) Jensen, A.; Hauptmann, J.; Nygård, J.; Sadowski, J.; Lindelof, P. *Nano Lett.* **2004**, *4*, 349.
(12) Javey, A.; Wang, Q.; Kim, W.; Dai, H. *IEEE Int. Electron Devices Meet.* **2003**, 32.2.132.2.4.
(13) Riben, A. R.; Feucht, D. L. *Solid-State Electron.* **1966**, *9*, 1055.
(14) Zeidenbergs, G.; Anderson, R. L. *Solid-State Electron.* **1967**, *10*, 113.
(15) Anderson, R. L. *Solid-State Electron.* **1962**, *5*, 341.
(16) Sze, S. M. *Physics of Semiconductor Devices*; Wiley: New York, 1981.
(17) Varshni, Y. *Physica* **1967**, *34*, 149.
(18) Capaz, R. B.; Spataru, C. D.; Tangney, P.; Cohen, M. L.; Louie, S. G. *Phys. Rev. Lett.* **2005**, *94*, 036801.
(19) Simon, F.; Pfeiffer, R.; Kuzmany, H. *Phys. Rev. B* **2006**, *74*, 121411.
(20) Appenzeller, J.; Radosavljević, M.; Knoch, J.; Avouris, Ph. *Phys. Rev. Lett.* **2004**, *92*, 048301.
(21) Tian, B.; Zheng, X.; Kempa, T. J.; Fang, Y.; Yu, N.; Yu, G.; Huang, J.; Lieber, C. M. *Nature* **2007**, *449*, 885.
(22) Law, M.; Greene, L. E.; Johnson, J. C.; Saykally, R.; Yang, P. *Nat. Mater.* **2005**, *4*, 455.
(23) Gratzel, M. *Nature* **2001**, *414*, 338.

NL0802178